



Ohmic lines for one-dimensional in-line and two-dimensional cylindrical Josephson junctions

Helweg, C.; Levring, O. A.; Samuelsen, Mogens Rugholm; Olsen, O.H.

Published in:
Journal of Applied Physics

Link to article, DOI:
[10.1063/1.335278](https://doi.org/10.1063/1.335278)

Publication date:
1985

Document Version
Publisher's PDF, also known as Version of record

[Link back to DTU Orbit](#)

Citation (APA):
Helweg, C., Levring, O. A., Samuelsen, M. R., & Olsen, O. H. (1985). Ohmic lines for one-dimensional in-line and two-dimensional cylindrical Josephson junctions. *Journal of Applied Physics*, 57(11), 5024-5027.
<https://doi.org/10.1063/1.335278>

General rights

Copyright and moral rights for the publications made accessible in the public portal are retained by the authors and/or other copyright owners and it is a condition of accessing publications that users recognise and abide by the legal requirements associated with these rights.

- Users may download and print one copy of any publication from the public portal for the purpose of private study or research.
- You may not further distribute the material or use it for any profit-making activity or commercial gain
- You may freely distribute the URL identifying the publication in the public portal

If you believe that this document breaches copyright please contact us providing details, and we will remove access to the work immediately and investigate your claim.

Ohmic lines for one-dimensional in-line and two-dimensional cylindrical Josephson junctions

C. Heiweg, O. A. Leving, and M. R. Samuelsen

Physics Laboratory I, The Technical University of Denmark, DK-2800 Lyngby, Denmark

O. H. Olsen

NIRO Atomizer, Systems Engineering, Gladsaxevej, DK-2860 Soeborg, Denmark

(Received 15 October 1984; accepted for publication 29 October 1984)

Expressions for the ohmic lines in the IV characteristic for one-dimensional in-line geometry Josephson junctions as well as for two-dimensional cylindrical Josephson junctions are presented. The expressions are compared to numerical simulations of Josephson junctions using the fluxon model; the ohmic line in this model corresponds to a continuous generation at the boundaries of fluxons and antifluxons, being pairwise annihilated in the middle (due to damping). For large currents the results fit to the expressions. Further we find that the fluxon generation in most cases were simply periodic; however, depending on the initial conditions we find 1/2 and 1/3 harmonic generation.

I. INTRODUCTION

The propagation of fluxons (magnetic flux quanta) in long and narrow Josephson junctions is still attracting research interest. The fluxon propagation has been convincingly shown to be responsible for the appearance of zero field steps (ZFS) and Fiske steps in the dc-current-voltage characteristics of such junctions.¹⁻⁴ Furthermore, emission of microwave radiation from the ends of the junctions is associated to this propagation which suggests the possibility of interesting electronic applications.

So far attention has primarily been given to junctions of overlap type in which the bias current is fed to the junction perpendicular to its long direction. As a first approximation the bias current is assumed to be distributed uniformly along the length of the junction. In the in-line geometry junction the current is fed in the long direction of the junction giving rise to self-fields which provide the energy input. In the limit of very short junctions, distinctions between geometries disappear.³ Further for very long junctions it has been shown in Ref. 5 that many features of the two geometries such as ZFS are quite similar. An attempt to model junctions of mixed overlap-in-line geometry has been performed in Ref. 6. This model agrees with experiments which show that the maximum supercurrent depends linearly on external magnetic fields. The so-called "linear displaced branch"⁷ which has been found experimentally has been ascribed to the mechanism which is modelled by the in-line geometry model. Finally, we mention the tunable oscillator proposed in Ref. 8 which is based on the idealized assumptions of a spatially uniform bias current which in a real junction is impossible to maintain since skin currents are set up which cancel the bias current from the inside of the junction.

The purpose of the present paper is to examine numerically the so-called ohmic line in long and narrow Josephson junctions of in-line geometry type as well as in large area circular Josephson junctions by means of the fluxon model. In the IV characteristic the zero-voltage current corresponds to a static fluxon at one end and a static antifluxon at the other which only partly have penetrated the junction. The ZFS correspond to fluxons propagating through the

junction each fluxon being reflected at the ends, while the ohmic line corresponds to a continuous generation of fluxons at one end and of antifluxons at the other end moving towards the center of the junction, where the fluxons and the antifluxons annihilate (due to the damping). The outline of the paper is as follows: in Sec. II we present the model; Sec. III contains the analysis which gives an approximate expression for the ohmic line, while Sec. IV contains the numerical results and comments. Finally in Sec. V we conclude.

II. THE MODEL

A Josephson tunnel junction is modelled by the perturbed sine-Gordon equation

$$\nabla^2 \phi - \phi_{tt} = \sin \phi + \alpha \phi_t, \quad (1)$$

where $\phi(\bar{r}, t)$ is the space and time dependent phase difference between the two superconducting films. The gradient term is two dimensional and has no components normal to the overlapping area of the junction. The spatial variable \bar{r} is measured in units of the Josephson penetration depth $\lambda_J = (\hbar / \mu_0 2edj_J)^{1/2}$ and the time t in units of the reciprocal plasma frequency ω_p^{-1} , $\omega_p = (2ej_J / \hbar C)^{1/2}$. Here $-e$ is the electron charge, $2\pi\hbar$ is Planck's constant, μ_0 is the permeability of free space, j_J is the maximal Josephson current density through the barrier, d is the magnetic thickness of the barrier ($2\lambda_L + t_0$), λ_L being the London penetration depth and t_0 the electric thickness of the oxide layer, C is the capacitance per unit area of the junction. The second term on the right-hand side of Eq. (1) represents dissipative effects. Thus $\alpha = G_0(\hbar / 2ej_J C)^{1/2}$, where G_0 is the conductance due to the quasiparticle tunneling current. G_0 is a fairly complicated function of voltage and temperature, but in the following we regard it as independent of voltage.

For a junction of one dimensional in-line geometry³ the current is fed to the junction in the long direction of the junction and for this situation the model Eq. (1) becomes

$$\phi_{xx} - \phi_{tt} = \sin \phi + \alpha \phi_t, \quad (1a)$$

with the boundary conditions

$$\phi_x(\pm l/2) = \frac{\pm I}{2W\lambda_{JJ}} \triangleq \pm \kappa. \quad (2)$$

Here we have chosen x to be the spatial variable in the long direction of the junction. $-l/2 \leq x \leq l/2$, where l is the normalized length of the junction. I is the total current flowing in the junction and W is the width of the junction. Equation (2) reflects that the current due to the so-called self-field effects is confined to an area of $2W\lambda_J$ at each end of the junction, and the current flowing in the junction only enters through the magnetic fields it creates at the ends, i.e., the boundary conditions.

For the cylindrical inline junction, which essentially is also an inline geometry junction the Eq. (1) due to the radial symmetry becomes

$$\phi_{rr} + (1/r)\phi_r - \phi_{\theta\theta} = \sin \phi + \alpha\phi_t, \quad (1b)$$

with the boundary conditions

$$\phi_r(r=R) = \frac{I}{2\pi R\lambda_{JJ}} \triangleq \kappa, \quad (3a)$$

$$\phi_r(r=R_i) = 0, \quad (3b)$$

where r is the radial variable $R_i \leq r \leq R$, R is the outer radius of the junction, R_i allows for a hole in the center of the junction of radius R_i . Equation (3) reflects that the current flows in a ring of width λ_J at the circumference of the junction.

III. ANALYSIS

A. Zero field steps (ZFS)

As mentioned above it is now possible to calculate the detailed structure of the first ZFS in an 1D in-line junction, using perturbation techniques. The detailed picture for the fluxon resonance is as follows (see Fig. 1). Due to the ohmic losses, the fluxon velocity will decrease when the fluxon travel from one end to another. When the fluxon reaches the boundary, it is reflected as an antfluxon travelling in the opposite direction, and during the reflection it receives an energy input from the magnetic field at the end. When the

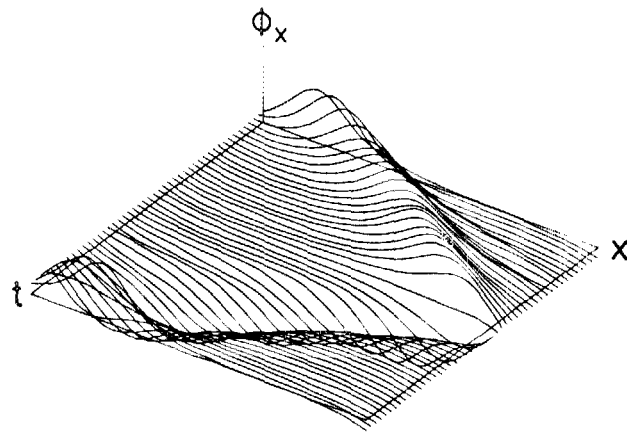


FIG. 1. Illustration of the fluxon propagation in a point on the first zero field step for the in-line geometry junction, parameter values are $\kappa = 0.5$, $\alpha = 0.1$, and $l = 10$. The mechanism mentioned in the text is clearly demonstrated.

antfluxon reaches the opposite end of the junction it is reflected as a fluxon with an increased energy and so forth. Combining the energy inputs at the ends with the equation of motion of a fluxon and neglecting the phaseshift the fluxon receives at the ends yields the following connection between current κ and the average velocity u of the fluxon, i.e., the dc voltage⁵

$$\kappa = \frac{4 \sinh(\alpha l/2)}{\pi \sqrt{\left(\frac{\tanh(\alpha l/2u)}{\tanh(\alpha l/2)}\right)^2 - 1}}. \quad (4)$$

From this we find that if the total damping of a fluxon αl exceeds the value ≈ 2.1 the resonance is not possible.

For the cylindrical in-line geometry it has so far not been possible to find either approximate solutions or experimental evidence for ZFS although approximate⁹ and numerical fluxon solutions¹⁰ are known.

B. Ohmic line

If the junction is biased on the zero-voltage current and the current is increased above the critical current of the junction, the junction will switch to a voltage state.

For the one dimensional in-line geometry the maximum zero-voltage current is given by $\kappa = 2$, i.e., $-\phi_x(x = -l/2) = \phi_x(x = l/2) = 2$. This magnetic field can be regarded as part of a stationary fluxon from the end into the junction. Since the maximum value of ϕ_x for a stationary fluxon is 2, an increase of κ above this value, will result in a continuous generation of fluxons at $x = l/2$ and of antfluxons at $x = -l/2$. The fluxons and antfluxons will annihilate in the center, and we end up with a steady state where fluxons and antfluxons are generated at constant rates depending on κ and subsequently are annihilated in the center. If we assume that the phase changes very fast with a constant angular velocity, i.e., $\alpha\phi_t \gg 1$ and $\phi_t = \omega$, we may ignore the $\sin \phi$ term in Eq. (1) and we get

$$\phi_{xx} = \alpha\omega. \quad (5)$$

Integrating this equation we get with the boundary conditions (2)

$$\phi_x = \alpha\omega x, \quad (6a)$$

which yields the asymptote in the dc-current-voltage characteristic

$$\kappa = (\alpha l/2) \langle \phi_t \rangle \quad (6b)$$

being the ohmic line for a one-dimensional inline junction.

For the cylindrical in-line the maximum zero-voltage current is given by $\kappa = 2$ as well. When the current is increased above this value, there will be a continuous generation of fluxons at the circumference of the junction. At the center of the junction, or allowing for a hole in the center of the junction, at the inner radius of the junction R_i , $\phi_r = 0$, a fluxon is reflected as an antfluxon, which annihilates another fluxon. In the limit $\alpha\omega \gg 1$ with the same assumption as above, Eq. (1b) turns into

$$\phi_{rr} + \frac{\phi_r}{r} = \alpha\omega, \quad (7a)$$

or

$$\frac{1}{r} \frac{\partial}{\partial r} (r \phi_r) = \alpha \omega, \quad (7b)$$

which may be integrated and combined with the boundary conditions $\phi_r(r = R_i) = 0$ and $\phi_r(r = R) = \kappa$ into

$$\kappa = \frac{\alpha}{2} \omega \frac{(R - R_i)(R + R_i)}{R}, \quad (8)$$

or with $R_i = 0$,

$$\kappa = \frac{\alpha R}{2} \langle \phi_t \rangle, \quad (9)$$

which is quite similar to Eq. (6b).

IV. NUMERICAL RESULTS AND COMPARISONS

In order to illustrate the fluxon mechanisms and the results obtained above we have composed numerical experiments of situations for various values of κ , thus we solve the initial value problem Eq. (1) with the boundary conditions in Eqs. (2) and (3) for the two geometries, respectively.

The voltage $\langle \phi_t \rangle$ is determined by measuring $\phi(t)$ in an arbitrary point, waiting for the solution to be stable, where the stability condition is that the time interval between each 2π charge of the phase for two subsequent periods did not deviate more than the time discretization.

A. 1D inline junction

In order to use the model of the one-dimensional in-line junction we solve Eq. (1a) applying the boundary conditions in Eq. (2). In Fig. 1 we illustrate the resonant fluxon propagation in a point on the first zero field step. Parameter values are $\kappa = 0.5$, $\alpha = 0.1$, and $l = 10$. The mechanism has been described above. In Fig. 2 we show fluxon-antifluxon generation, propagation and annihilation in a point on the ohmic line, as described above. Parameter values are $\kappa = 2.3$, $\alpha = 0.1$, and $l = 10$. In this case the simulations have been performed by solving only the half of the line applying the boundary conditions $\phi_x(0, t) = 0$ and $\phi_x(l/2, t) = \kappa$.

The ohmic lines obtained by simulation and from the approximated expressions are shown in Fig. 3. In the limit

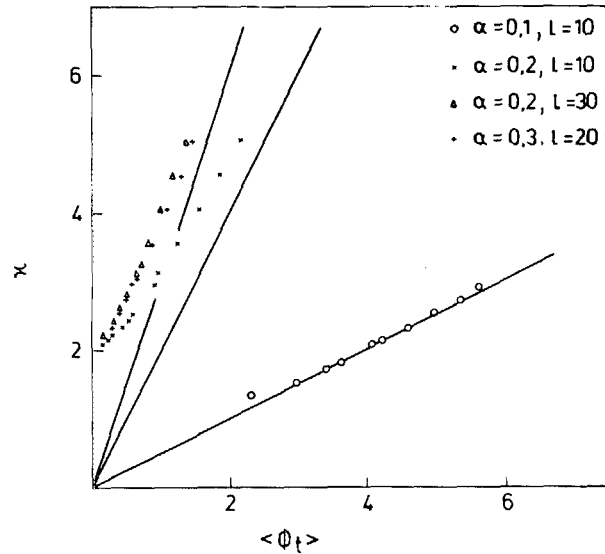


FIG. 3. Comparison between the approximated expression for the ohmic line in an in-line geometry junction and numerical simulations. The full lines are the expression Eq. (6). The results for $\alpha l = 1$ where $\kappa < 2$ were found using the initial conditions $\phi_i(x, 0) = 2\kappa/\alpha l$. For large currents ($\kappa \gg 1$) the expression fits very well the simulations.

$\kappa \gg 2$ the numerical results fit very well with the expression in Eq. (6b). The results obtained for $\kappa < 2$ are found using the initial condition $\phi_i(x, 0) = 2\kappa/\alpha l$. Although the mechanism behind the ohmic line is the same as the one suggested for explaining the so-called "resistive branch," our calculations show a curvature similar to the so-called "Stewart-McCumber" curves for small tunnel junctions, rather than a strictly linear slope. There may be several reasons for this. One may be that we did not have proper initial conditions for the simulation. Another reason may be that the "resistive branch," is not contained in the model Eq. (1a) as we do not have the proper nonlinear quasi-particle resistance. A third suggestion¹¹ which has come forward quite recently is that the "resistive branch" may be due to shorts in the junction. The latter suggestion was based on experiments where it was observed that the junctions exhibiting this phenomenon all

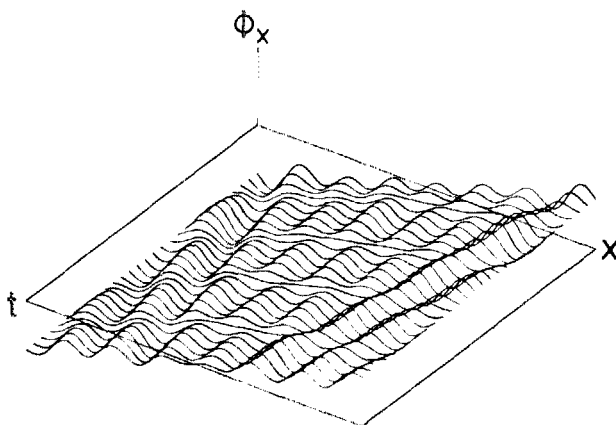


FIG. 2. Fluxon-antifluxon propagation in a point on the ohmic line. Fluxons and antifluxons are generated at the ends and annihilated in the middle. Parameter values are $\kappa = 2.3$, $\alpha = 0.1$, and $l = 10$.

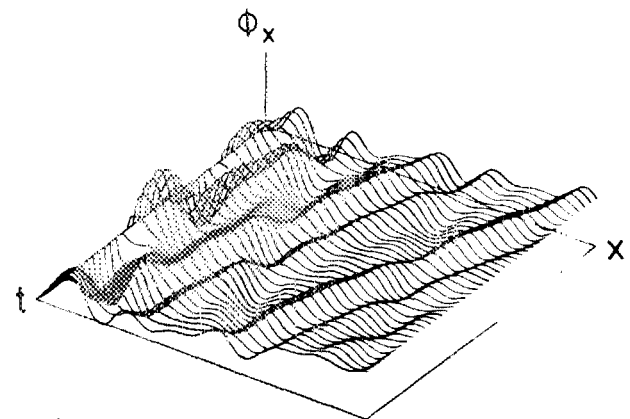


FIG. 4. Illustration of the fluxon-antifluxon propagation in a two-dimensional circular junction. Fluxons are generated at the outer radius of the junction, reflected at the center as an antifluxons which annihilates another fluxon. Parameter values are $\kappa = 2.3$, $\alpha = 0.1$, $R_i = 0$, and $R = 10$.

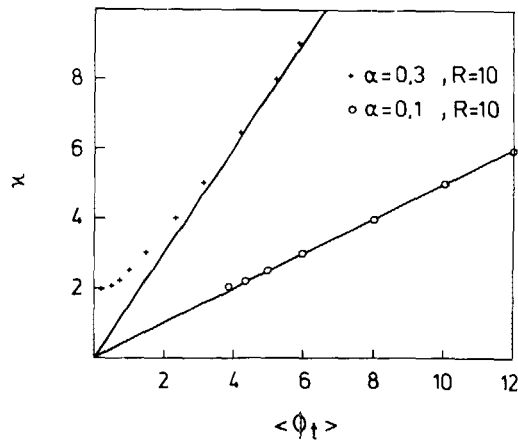


FIG. 5. Comparison between the approximated expression for the ohmic line in a 2D circular junction and numerical simulations. The full lines are the expression Eq. (8). There is good agreement between the expression and the simulations.

have an unexpectedly high current density when being compared to small junctions with the same fabrication data.

In most cases the fluxon-antifluxon generation was simply periodic meaning that the time deviation between each 2π change of ϕ was given only by the time discretization. For curiosity, however, we mention that, depending on the initial conditions, we in some cases found two alternating time intervals between each 2π change in ϕ and even sequences with three different intervals, corresponding to $1/2$ and $1/3$ harmonic generation, respectively. Both of these situations seemed to be stable.

Finally we note that for $\alpha l = 1$ we found a hysteretic behavior of this "Stewart-McCumber" curve.

B. 2D cylindrical junction

For the 2D cylindrical junctions we have also simulated the ohmic line by solving Eq. (1b) with the boundary conditions Eq. (3). In Fig. 4 we illustrate the fluxon generation mechanism in a point on the ohmic line. The mechanism is

described above. The parameter values are $\kappa = 2.3$, $\alpha = 0.1$, $R_i = 0$, and $R = 10$. In Fig. 5 the ohmic lines obtained by numerical simulation and from the expression Eqs. (3) for $R_i = 0$ are shown. We observe a good agreement between analysis and simulation for $\kappa \gg 2$.

We note that for $R_i = 0$ no ZFS has been found, while for $R_i \gg 1$ (where $\phi_r/r \ll 1$) the 1D and 2D junctions act quite similar.

V. CONCLUSION

In the present paper we have presented results for ohmic lines obtained from the fluxon model. An asymptotic expression for the ohmic line is presented for 1D and 2D junctions. Comparisons between the expressions and results obtained by numerical simulation of the model show good agreement for large currents.

The "resistive branch" which has been explained by the 1D inline geometry model has not been found; possible explanations for this have been given.

Detailed studies of the 1D model shows that the fluxon generation is simply periodic. However, generation of $1/2$ and $1/3$ harmonics have been found.

¹S. N. Ern  and R. D. Parmentier, J. Appl. Phys. **51**, 5025 (1980).

²P. S. Lomdahl, O. H. Soerensen, and P. L. Christiansen, Phys. Rev. B **25**, 5737 (1982).

³S. N. Ern , A. Ferrigno, and R. D. Parmentier, IEEE Trans. Magn. **MAG-19**, 100 (1983).

⁴B. Dueholm, O. A. Levring, J. Mygind, N. F. Pedersen, O. H. Soerensen, and M. Cirillo, Phys. Rev. Lett. **46**, 1299 (1981).

⁵O. A. Levring, N. F. Pedersen, and M. R. Samuelsen, Appl. Phys. Lett. **40**, 846 (1982); J. Appl. Phys. **54**, 987 (1983).

⁶O. H. Olsen and M. R. Samuelsen, J. Appl. Phys. **54**, 6522 (1983).

⁷A. C. Scott and W. J. Johnson, Appl. Phys. Lett. **14**, 316 (1969).

⁸P. L. Christiansen, P. S. Lomdahl, and N. J. Zabusky, Appl. Phys. Lett. **39**, 170 (1981).

⁹M. R. Samuelsen, Phys. Lett. **74A**, 21 (1979).

¹⁰P. L. Christiansen and O. H. Olsen, Phys. Scr. **20**, 531 (1979).

¹¹M. Radparvar and J. E. Nordman, IEEE Trans. Magn. **MAG-17**, 796 (1981).